International Communications in Heat and Mass Transfer 161 (2025) 108406

Contents lists available at ScienceDirect

International Communications in Heat and Mass Transfer

journal homepage: www.elsevier.com/locate/ichmt

Thermal-frictional behavior of solid magnetic strip turbulator and helical coiled wire turbulator inside a double tube heat exchanger

Nemat Mashoofi Maleki [a], Saman Pourahmad [b,c], Ebrahim Tavousi [d], Noel Perera [d,*], Pouyan Talebizadehsardari [e], Amir Keshmiri [f]

[a] Faculty of Mechanical and Energy Engineering, Shahid Beheshti University, Tehran, Iran
[b] SuperPipe International, Tehran, Iran
[c] Department of Mechanical Engineering, Faculty of Engineering, Urmia University, Urmia, Iran
[d] College of Engineering, Faculty of Computing, Engineering and the Built Environment, Birmingham City University, Birmingham B4 7XG, UK
[e] Power Electronics, Machines and Control (PEMC) Group, University of Nottingham, Nottingham, UK
[f] School of Engineering, University of Manchester, Manchester, UK

ARTICLE INFO

Keywords:
Double tube heat exchanger
Heat transfer coefficient
Pressure drop
Magnetic turbulator
Helical coiled wire
Thermal efficiency

ABSTRACT

In recent years, the magnetic turbulator, which employs an electromagnetic vibration (EMV) technique, has gained popularity for its effectiveness in enhancing heat transfer within heat exchangers. This study introduces a novel approach by using solid strips instead of traditional flexible strips to construct solid magnetic strip turbulators (SMST) for the first time. Additionally, a helical coiled wire turbulator (HCWT) was combined with the SMST to investigate the synergistic effects of active and passive methods. Tests were conducted on SMST with various strip widths ranging from 5 to 7 mm and at different flow rates ranging 0.5 to 4 l/min, extensively analyzing the thermal-frictional parameters. The results revealed that the oscillating motion of the SMST induced higher turbulence near the tube wall compared to traditional turbulators. Moreover, an increase in strip width led to higher heat transfer coefficient and friction factor levels. When SMST and HCWT were used independently, heat transfer increased by up to 311 % and 201 %, respectively. When used together, heat transfer coefficient and friction factor increased by up to 6.55 and 3.85 times those of a plain tube, respectively. In an optimal scenario, the thermal efficiency factor increased to 4.18.

1. Introduction

A heat exchanger is an apparatus that allows for the transfer of thermal energy (enthalpy) between multiple fluids, separated by a solid medium. These devices are integral to numerous industrial applications, where they are employed for processes such as crystallization, concentration, distillation, fractionation, pasteurization, sterilization, and the control of process fluids. These applications span power plants, electronics, chemical and food industries, cooling towers, waste heat recovery, air-conditioning systems, condensers, automobile radiators, and space-related applications [1]. Among the various types of heat exchangers available, one of the most commonly used heat exchangers that exhibit low design, installation, and maintenance costs is the double tube heat exchanger (DTHE) [2]. Improving the performance of heat exchangers and increasing heat transfer rates can lead to enhanced efficiency and higher productivity in all the aforementioned industries. Enhancing the heat transfer in heat exchangers can be achieved through three primary methods: passive, passive, or compound. The objective of passive methods is to improve the heat transfer rate independently of any external energy influences. These methods involve incorporating various techniques to induce turbulence in the flow, such as inserting fins, coiled wires, inducing swirl flow, and introducing wall roughness [3–6]. Enhancing heat transfer techniques through passive methods is crucial not only in heat exchangers but also in heat sinks, which are essential devices for heat dissipation [7–11]. Conversely, the active method employs external energy to enhance the rate of heat transfer [12–14]. The compound method refers to the combined utilization of passive and active methods to enhance the heat transfer rate and overall performance of the heat exchangers [15,16]. In a broad sense, active methods can be classified into four distinct sections: mechanical aid, electrohydrodynamic (EHD), magnetohydrodynamic (MHD), and pulsating flow. To augment the heat transfer rate through the application of

* Corresponding author.
E-mail address: noel.perera@bcu.ac.uk (N. Perera).

https://doi.org/10.1016/j.icheatmasstransfer.2024.108406

Available online 7 December 2024

mechanical aid techniques, it is imperative to disrupt the thermal boundary layer adjacent to the heated surface. This objective can be accomplished by inducing flow motion or agitation through the utilization of mechanical power [17]. EHD methods utilize electric fields to enhance heat transfer by inducing motion in dielectric fluid. By applying low current and high voltage, the electric energy is converted into kinetic energy, increasing fluid motion and disrupting the boundary layer, resulting in improved heat transfer [18–20]. MHD is a method that utilizes magnetic fields to influence the behavior of magnetic fluids, known as ferrofluids, which are colloidal solutions containing magnetic nanoparticles. By applying a magnetic field, the flow of ferrofluids, made up of nano-sized particles such as magnetite and carrier fluids like water or oils, can be easily controlled and manipulated [21–23]. Pulsating flow is a technique similar to mechanical assistance that entails the application of oscillating motion to the heat transfer fluid. This motion serves to disrupt the thermal boundary layer and enhance heat transfer. Extensive research has been conducted on pulsating flow, confirming its effectiveness in improving heat transfer by facilitating the exchange of vortexes with the main flow [24–26].

Maleki, et al. [27] experimentally conducted a novel active method to evaluate the heat transfer rate in a heated tube. A string was coaxially inserted inside the heated tube that induced vibration at its natural frequency using an AC magnetic field. They called it the electromagnetic vibration method (EMV). By varying both the diameter of the vibrating string and the location of the excitation along the tube, they investigated the impact on radial and turbulence flow effects. The results indicated that positioning the stimulation point at a distance of one-third from the outlet of the heated tube notably increased the heat transfer, ultimately reaching the optimal level. They also found that increasing the diameter of the vibrating string contributed to a significant rise in the heat transfer rate, particularly at lower mass flow rate conditions. Maleki, et al. [28] assessed the heat transfer characteristics of a horizontal tube with the inclusion of vibrating oscillator turbulators through experimental and numerical investigations. The research investigation centered on examining the effects of varying vibrational frequencies on heat transfer coefficients in two distinct geometries: vibrating string and strip. The findings clarified that the vibrating string oscillator exhibited a notable enhancement of 110 % in the heat transfer coefficient, while the vibrating strip oscillator demonstrated a substantial increase of 150.3 % in the Nusselt number. Additionally, it has been noted that increasing the vibration frequency improves the thermal performance. Khedher, et al. [29] introduced a vibrating woven wire turbulator to improve the thermal efficiency of DTHEs. Experiments in laminar and turbulent flows (Re = 1000–8500) showed a 236 % increase in heat transfer with minimal pressure drop. Combining it with a helical coiled wire turbulator (HCWT) improved heat transfer by 545 %, achieving a thermal enhancement factor (TEF) of 3.13. Yao, et al. [30] evaluated the effect of using magnetic and HCW turbulators, both individually and together, in a DTHE. Results showed that the simultaneous use of both turbulators improves heat transfer by up to 5.9 times, achieving a TEF of 3.78. The optimal pitch ratio for HCW was found to be 5. Pan, et al. [31] investigated the use of perforated magnetic turbulators in DTHEs to enhance heat transfer. Various perforation diameters, pitch, and flow rates were evaluated. Results showed that simple and perforated turbulators increased heat transfer by 156 % and 150 %, respectively, with a maximum TEF of 2.06 for a turbulator with a 2 mm diameter and 12 mm pitch. Abed, et al. [32] evaluated the combined effect of bubble injection and a magnetic turbulator on the thermal efficiency of a DTHE. Experiments showed heat transfer improvements of 150.3 % with bubble injection, 328.8 % with the turbulator, and 586.2 % when both are used together. The optimal configuration achieved a TEF of 3.45, with increased friction factors observed in all cases.

Zohir, et al. [33] conducted an experimental study to investigate the effect of helically coiled wire insertion within the outer tube of a DTHE. The Reynolds number ranged from 4000 to 14,000, with hot water at 65 °C flowing through the inner tube and cold water at 25 °C circulating in the outer tube. The findings indicated a substantial rise in heat transfer efficiency, with increases of up to 450 % and 400 % for counterflow and parallel flow configurations, respectively. It was also concluded that the Nusselt number increased with higher Reynolds numbers and lower pitch ratios. Akpinar [34] Executed an experimental analysis to determine the influence of HCWT on thermal-frictional characteristics within a DTHE. The Reynolds number ranged from 6500 to 13,000, with hot air and cold water employed as the working fluids in the inner and outer tubes, respectively. The results revealed significant improvements in the Nusselt number and friction factor, with increases of up to 164 % and 174 %, respectively, in comparison to a plain DTHE. Padmanabhan, et al. [35] carried out a numerical analysis focusing on the insertion of HCWT in a DTHE to investigate its effects on hydrothermal properties. They utilized cold water at 28 °C within the inner tube and hot water at 90 °C within the outer tube. The outcomes of this numerical investigation demonstrated an enhancment of up to 63.91 % in the Nusselt number and an increase in heat flux by reducing the pitch ratio of the coiled wire.

Several studies have investigated different parameters concerning the EMV method, including the oscillator's geometry, perforation impact, and frequency [36]. Typically, a flexible wire or strip has been commonly used as the oscillator throughout these investigations. However, in the present investigation, a solid oscillator is utilized for the first time in the EMV method, allowing for an evaluation of its impact on the hydrothermal properties. By substituting a flexible oscillator with a solid one, the effectiveness of the EMV technique is expected to be enhanced. This is attributed to the solid oscillator's ability to direct a larger quantity of fluid toward the tube wall during specific geometric and vibrational movements. In contrast, the flexible strip turbulator only achieves maximum amplitude of vibration in a small portion of the strip, while the entire solid strip turbulator geometry vibrates at maximum amplitude within the tube. In addition, for the first time, a HCWT was also added to the tube to investigate the simultaneous effect of an active and passive method. By incorporating the wire into the pipe, the boundary layer near the wall is disrupted, while the central currents are propelled toward the pipe with the assistance of the magnetic turbulator. In investigating the thermal-frictional behavior, various parameters were considered, including the width of the oscillator, the flow rate of the inner tube, and the simultaneous use of an HCWT and SMST. Through a comprehensive analysis of different scenarios, the optimal combination was identified using the TEF. Subsequently, the findings of this investigation were compared to previously published literature.

2. Definition of the experimental setup

Fig. 1 illustrates a diagram of the experimental test rig, which includes multiple components, including a test section, a centrifugal pump, hot and cold water tanks, control valves, two flow meters, thermocouples, pressure gauges, and a data logger. The test section was a double-tube heat exchanger featuring an inner and outer tube made of copper. The inner and outer tube diameters were 16 mm and 25.4 mm respectively, with a length of 750 mm and 1 mm thickness. Insulation using glass wool and foam was applied around the outer tube to minimize heat losses. In this experimental setup, the working fluid was cold water flowing through the outer tube, while hot water was circulated through the inner tube concurrently. Four K-type thermocouples were used for temperature measurements to maintain constant inlet temperatures for hot and cold fluids. In the hot loop, a 100 W centrifugal pump and a 2 kW heater were employed to control the inlet temperature of the hot fluid at a constant temperature of 50 °C. Also, the temperature of the cold water was fixed at 20 °C. The hot water fluid entered the inner tube at a flow rate ranging from 0.5 to 4 l/min, corresponding to the Reynolds numbers 1050–8430, while the cold fluid was circulated through the annular space between the two tubes with a constant flow rate of 5 l/min. The flow rates of both hot and cold fluids were measured using a turbine and a pulse meter (Autonics M5P8w). All measurement devices

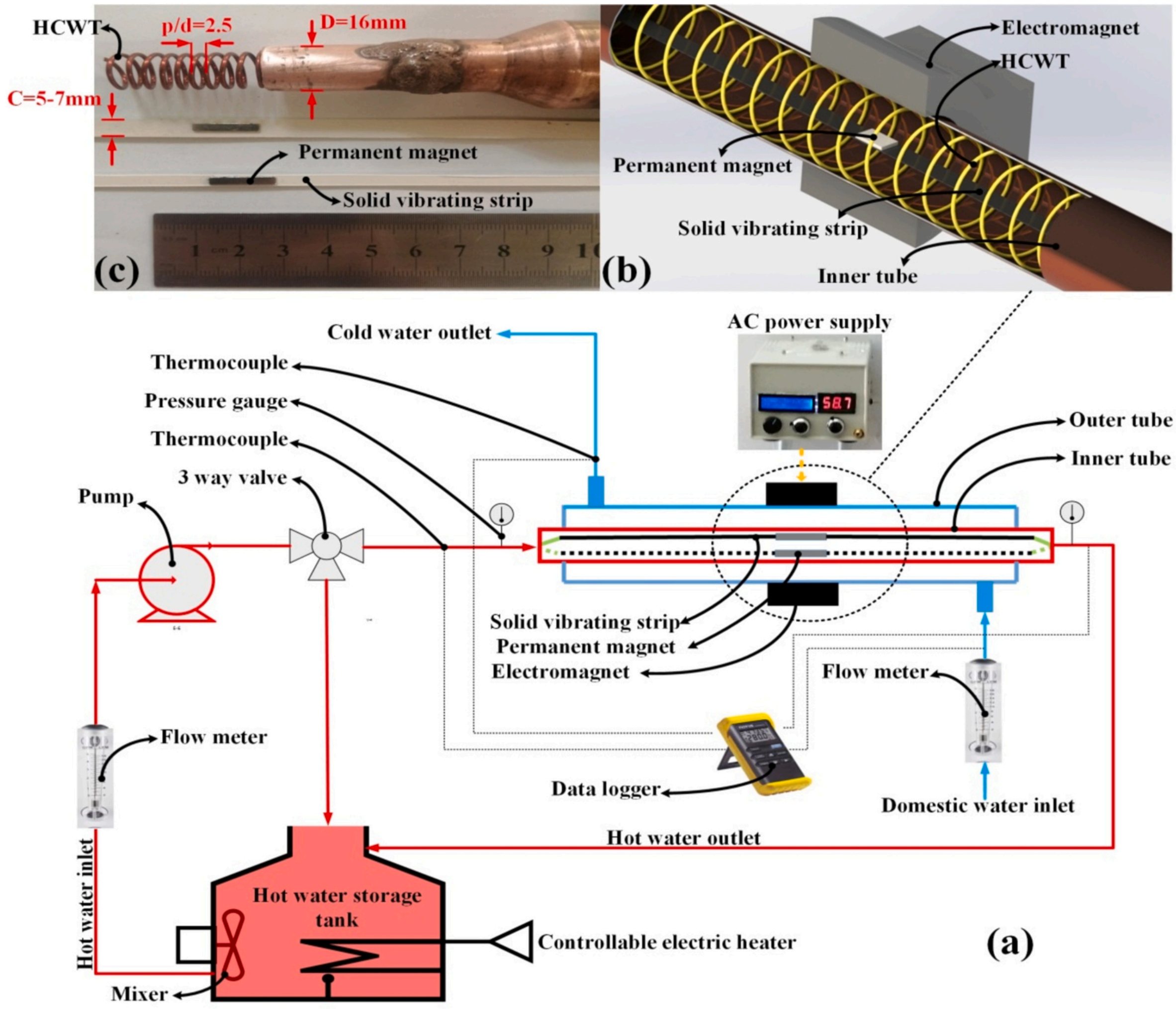

Fig. 1. (a) 2D illustration of the experimental setup (b) inside of the inner tube (c) dimensions of the solid strip and helical coiled turbulators.

were calibrated, and the experiment was conducted under steady-state conditions with a data acquisition system used to record the test data. This investigation examined two types of turbulator insertions to enhance heat transfer within the inner tube. The first method involved utilizing a helical coiled wire turbulator (HCWT) as a passive method, characterized by dimensions of 1 mm diameter and 2.5 mm pitch ratio. The second, an active method utilized a solid magnetic strip turbulators (SMST) option as an electromagnetic vibrator. This SMST has a length of 700 mm and a width ranging from 5 to 7 mm. Specifications of the test section, conditions, and turbulators are presented in Table 1. Also, Fig. 2 illustrates the distinction between an SMST and a traditional flexible strip. By employing the SMST, the solid strip undergoes simultaneous upward and downward movements, perfectly aligning with the horizontal plane. This action disrupts the fluid flow along the entire path. However, in the traditional flexible strip, the oscillation amplitude of the strip is variable. Near the ends of the tube, the amplitude of the oscillation decreases significantly, approaching zero, whereas it peaks at the center of the tube. The flexible strip's central section most significantly influences the flow patterns, contrasting with the solid strip's consistent impact throughout the tube. Therefore, it is expected that the effect of the SMST on heat transfer will be greater than the traditional flexible strip.

3. Data processing

The unprocessed data collected from the experiments encompasses the temperature readings from both the inlet and outlet, as well as the measurements of pressure drop within the test section. To convert these data to the heat transfer coefficient, friction coefficient, and finally, the TEF, the following process is carried out for all cases.

3.1. Inner tube heat transfer coefficient

To determine the heat transfer rate for both the inner and outer tubes (Q_h *and* Q_c) Eqs. (1) and (2) are employed.

$$Q_h = \dot{m}_h C_{p,w}\left(T_{h,i} - T_{h,o}\right) \tag{1}$$

$$Q_c = \dot{m}_c C_{p,w}\left(T_{c,o} - T_{c,i}\right) \tag{2}$$

In this context, $\dot{m}$ represents the mass flow rate, while C_p denotes the specific heat capacity of the working fluid. The designations i, o, h, and c correspond to the inlet, outlet, hot, and cold variables, respectively. It should be mentioned that the Q_h and Qc have a slightly different value, which could be due to the escape of energy from the insulation surface. The difference recorded in all tests was less than 3 %. To enhance the overall heat transfer accuracy and mitigate the error, the average of these two values was established according to Eq. (3). [37].

$$Q_{ave} = \frac{Q_c + Q_h}{2} = UA\Delta T_{LMTD} \tag{3}$$

Where U is the overall heat transfer coefficient, A is the inner tube surface area, and ΔT_{LMTD} is the logarithmic temperature difference. The

Table 1
Specifications of the test section, conditions, and turbulators.

Technical details of the test section	
Inner tube diameter (d)	16 mm
Outer tube diameter (D)	25.4 mm
Heat exchanger effective length (L)	750 mm
Tubes material	Copper
Tubes thickness	1 mm
Insulation material and thickness	glass wool, 20 mm
Heater capacity	2 kW
Technical details of SMST and HCWT	
Width of SMST	5–7 mm
Thickness of SMST	0.5 mm
Pitch ratio of HCWT (p/d)	2.5
SMST Material	Polycarbonate
Turbulator length	700 mm
HCWT wire diameter	1 mm
AC power supply and Electro-magnet specification	
Output Power	40 W
Input power	220 V-AC
Frequency range	10–600 HZ
Copper wire turns around the U-shape core	2500
Test condition	
Flow rate in the inner tube (hot water)	0.5 to 4 *l/m*
Flow rate in the outer tube (cold water)	5 *l/m*
Hot water inlet temperature	50 °C
Cold water inlet temperature	20 °C
Ambient Temperature	25 °C

inner tube surface can be evaluated by $A = \pi d_{in} L$. Also, the logarithmic mean temperature difference ΔT_{LMTD} is calculated using below Eq. (4) [37].

$$\Delta T_{LMTD} = \frac{(T_{h,i} - T_{c,o}) - (T_{h,o} - T_{c,i})}{Ln\frac{(T_{h,i}-T_{c,o})}{(T_{h,o}-T_{c,i})}} \quad (4)$$

To ascertain the inner surface heat transfer coefficient (h_i) of the inner tube, one may utilize the equation provided below [37].

$$\frac{1}{h_i} = \frac{1}{U} - \left(\frac{A_i ln(d_{ou} - d_{in})}{2\pi kL} + \frac{1}{h_o}\right) \quad (5)$$

Considering that the flow in the outer tube is turbulent (Re = 12,975), The evaluation of the heat transfer coefficient for the outer surface of the inner tube is conducted using the Dittus-Bolter Eq. (h_o). The Dittus-Boelter Eq. for heating flow is defined as follows [37]:

$$h_{ou} = 0.023 Re_{ou}^{0.8} Pr_{ou}^{0.4} \quad (6)$$

The equations listed below serve as a means to calculate the Reynolds and Prandtl numbers relevant to the outer tube.

$$Re_{ou} = \frac{\rho_{ou} V_{ou} D_{h,ou}}{\mu_{ou}} \quad (7)$$

$$Pr_{ou} = \frac{C_{p,ou}\mu_{ou}}{K_{ou}} \quad (8)$$

The variables $C_{p,ou}$, μ_{ou}, ρ_{ou}, K_{ou}, V_{ou}, and $D_{h,ou}$ represent the specific heat capacity, viscosity, density, thermal conductivity, velocity, and hydraulic diameter (D_{ou}-D_{in}), of the outer fluid. It's important to emphasize that the K_{ou} is calculated using the average of the inlet and outlet temperatures. In addition, the Reynolds number for the inner tube can be determined with the equation shown below [37].

$$Re = \frac{\rho_{in} V_{in} D_{h,in}}{\mu_{in}} \quad (9)$$

The inner fluid's dynamic viscosity, indicated by μ_{in}, is measured at the average temperature corresponding to the inlet and outlet. The friction factor coefficient (*f*) can be easily derived from the pressure drop data, as illustrated in the subsequent Eq. [37].

$$f = \frac{2D_h \Delta P}{L \rho V^2} \quad (10)$$

For a standard comparison of the examined scenarios (SMST, HCWT, and a combination of SMST and HCWT), the Thermal Enhancement Factor (TEF) was used. This variable concurrently evaluates variations in heat transfer and pressure drop, concerning baseline data from a standard tube. Thus, the TEF is instrumental in ascertaining an economically viable and optimal solution. The TEF can be calculated through the following equation. [38,39].

$$TEF = \frac{\frac{h}{h_{enhanced}}}{\left(\frac{f}{f_{enhanced}}\right)^{1/3}} \quad (11)$$

4. Uncertainty of measurement

Errors and uncertainties are inherent in experimental procedures and measurements, stemming from factors such as instrument accuracy and measurement processes. An evaluation of the uncertainty in independent parameters (*X1, X2, …, Xn*), which encompasses temperatures and flow rates, was conducted by taking into account the precision of the utilized instruments. In addition, the uncertainties related to the measurement parameters ($W_R^{\pm}$), specifically the heat transfer coefficient (*h*) and heat flux (q''), were analyzed. The following equation was used to calculate the uncertainties in the measurement parameters using the Moffat method [40,41]:

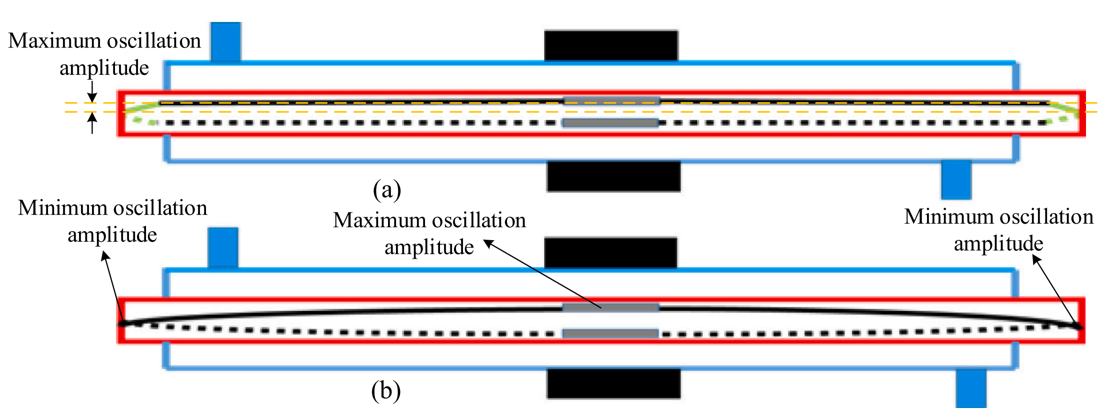

Fig. 2. Difference between traditional flexible strip and solid SMST motion (a) SMST (b) traditional flexible strip.

$$W_{R^+} = \left[\left(\frac{\delta \boldsymbol{R}^+}{\delta X_1} w_1\right)^2 + \left(\frac{\delta \boldsymbol{R}^+}{\delta X_2} w_2\right)^2 + \dots + \left(\frac{\delta \boldsymbol{R}^+}{\delta X_n} w_n\right)^2\right]^{\frac{1}{2}} \tag{12}$$

Where W_R^+ and W_n are dependent and independent variables of uncertainty, respectively. The resulting uncertainty in the heat transfer coefficient, friction factor, and Reynolds number were determined to be less than 5 %, 7 %, and 3 %, respectively, which are within an acceptable range. Table 2 presents the accuracy of the instruments used in the experiment. In addition, a demonstration of the calculation of uncertainty pertaining to the Reynolds number is outlined below.

$$Re = \frac{\rho \overline{V} D_H}{\mu} \tag{13}$$

$$W_{Re} = \left(\left(\frac{\delta Re}{\delta \rho} w_\rho\right)^2 + \left(\frac{\delta Re}{\delta \overline{V}} w_{\overline{V}}\right)^2 + \left(\frac{\delta Re}{\delta D_H} w_{D_H}\right)^2 + \left(\frac{\delta Re}{\delta \mu} w_\mu\right)^2\right)^{1/2} \tag{14}$$

By derivation we will have.

$$\frac{\delta Re}{\delta \rho} = \frac{\overline{V} D_H}{\mu}, \frac{\delta Re}{\delta \overline{V}} = \frac{\rho D_H}{\mu}, \frac{\delta Re}{\delta D_H} = \frac{\rho \overline{V}}{\mu}, \frac{\delta Re}{\delta \mu} = \frac{\rho \overline{V} D_H}{\mu^2} \tag{15}$$

Finally, by substituting relation 15 into relation 14, it can be written.

$$W_{Re} = \left(\left(\frac{\overline{V} D_H}{\mu} w_\rho\right)^2 + \left(\frac{\rho D_H}{\mu} w_{\overline{V}}\right)^2 + \left(\frac{\rho \overline{V}}{\mu} w_{D_H}\right)^2 + \left(\frac{\rho \overline{V} D_H}{\mu^2} w_\mu\right)^2\right)^{1/2} \tag{16}$$

5. Results and discussion

5.1. Validation

The heat transfer coefficient of a plain DTHE was compared to the empirical correlation proposed by Dittus-Boelter and Sieder-Tate [37,42]. Similarly, the friction factor of a plain DTHE was compared to the friction factors obtained from correlations provided by Petukhov [43]. Figs. 3 and 4 illustrate these comparisons for a range of mass flow rates against heat transfer coefficient and friction factor. The average deviations of the results from the correlations for the heat transfer coefficient and friction factor were below 6 % and 9 %, respectively.

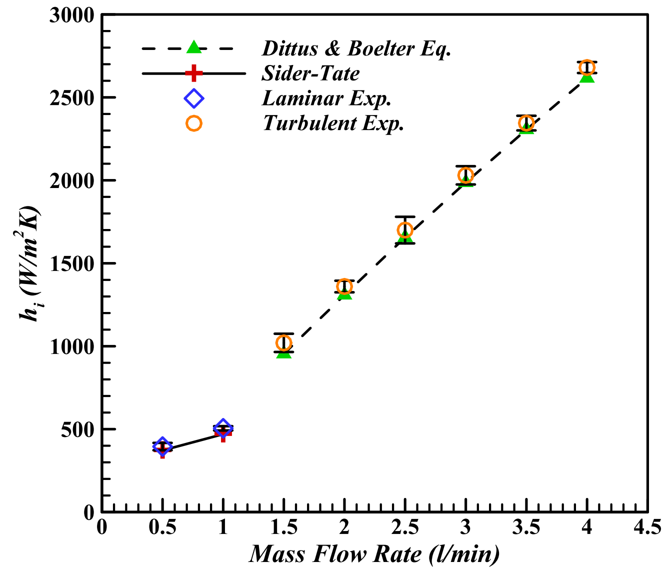

Fig. 3. Validation of heat transfer coefficient.

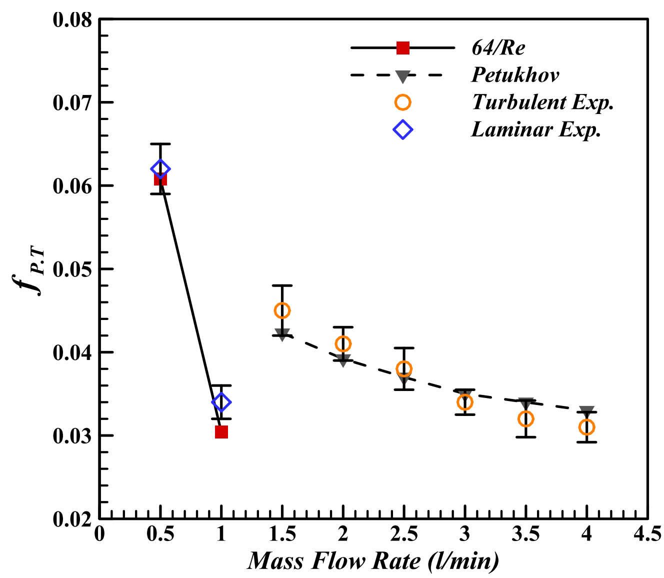

Fig. 4. Validation of friction factor.

5.2. Altering the oscillator width

In this study, for the first time, a solid strip was used to construct the solid magnetic strip turbulator (SMST). The thermal-frictional parameters were assessed by placing the SMST inside the inner tube of a heat exchanger. Experiments were performed for different SMST widths between C = 5 and C = 7 mm in the Reynolds number range of 1050 to 8430. The changes in the heat transfer coefficient (h_i) and the friction factor ratio (f/f_0) for the SMST with different widths are shown in Figs. 5 and 6, respectively. According to the results, the presence of the SMST with a width of 7 mm increased the h_i by 287 % to 61 % compared to the plain DTHE at Reynolds number ranging 1052 to 8430, respectively. By placing the SMST inside the tube, it reduced the tube space causing a reduction in the hydraulic diameter. This reduction in the hydraulic diameter caused an increase in the fluid velocity. Furthermore, the SMST causes vibrations inside the tube, leading to radial flows that enhance the collision of fluid particles with the tube wall, thus improving heat transfer. This distortion and weakening of the boundary layer significantly boost heat transfer compared to a plain DTHE. Fig. 6 also demonstrates that heat transfer rises with an increase in the width of the SMST. For instance, a C = 7 mm SMST at Reynolds number of 1054 can result in up to 33 % higher heat transfer compared to a C = 5 mm SMST. Wider SMST obviously increases the contact surface area with the fluid, hence affecting the flow path and intensifying radial flows, ultimately enhancing heat transfer.

Furthermore, the turbulator introduces a force in the opposite direction to the flow's path, resulting in an increase in the friction factor. The results show that the maximum pressure drop is observed for the SMST C = 7 mm width. The friction factor with the SMST C = 7 mm changes from 1.85 to 1.22 while for a C = 5 mm the friction factor

Table 2
Accuracy of the instruments.

Parameters to be measured	Measurement apparatus	Accuracy range in the catalog
Working fluid flow rate	AUTONICS Mp5 + puls meter	±2 %
Pressure drop	PAKKENS	±4 %
Temperature (data logger)	TES 1384	±0.5 %
Temperature (thermocouple)	K-type thermocouple	±0.5 %

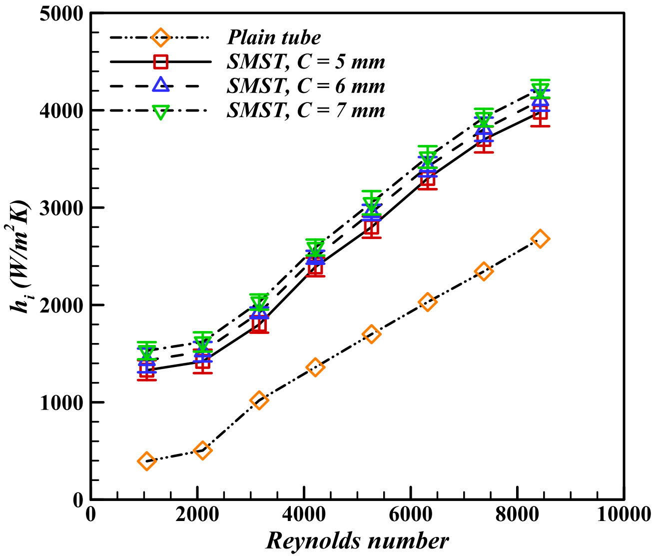

Fig. 5. h_i against Reynolds number for different SMST widths.

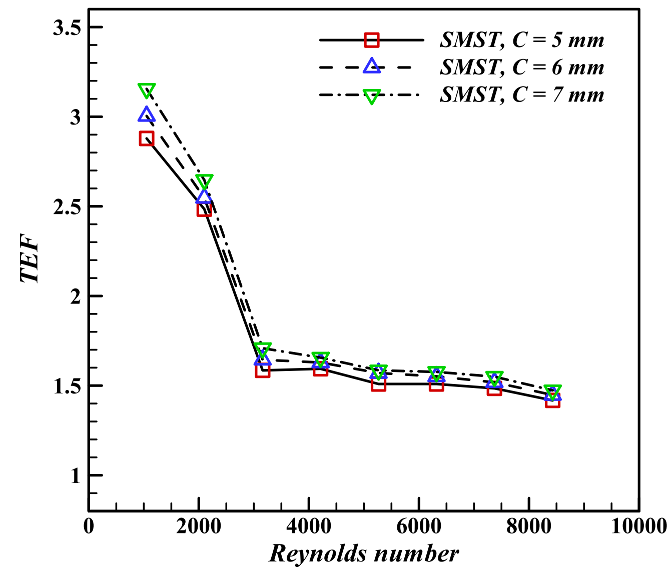

Fig. 7. TEF against Reynolds number for different SMST widths.

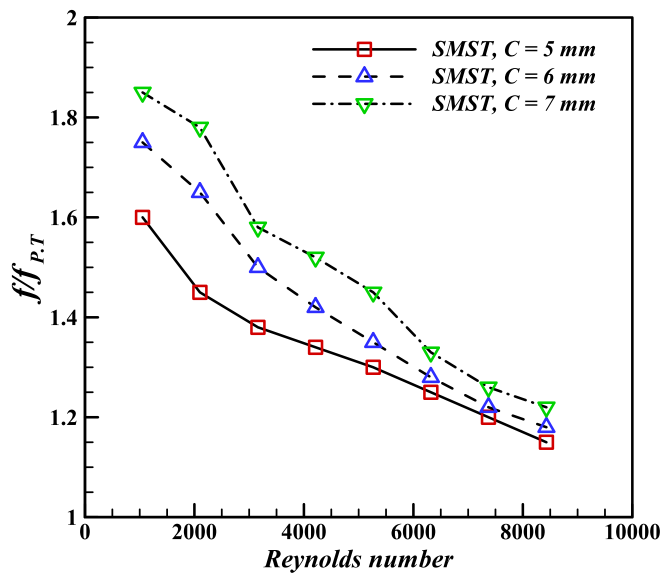

Fig. 6. f/f_0 against Reynolds number for different SMST widths.

changes in the range of 1.6 to 1.15 at Reynolds number ranging 1052 to 8430, respectively. The SMST positively affects the heat transfer and negatively affects the pressure drop. The changes in TEF with the Reynolds number for SMST with different widths are shown in Fig. 7. As shown, the TEF value exceeds one for all SMST widths ranging from 5 mm to 7 mm, indicating satisfactory performance. Also, according to the results, TEF increases with an increase in the SMST width. The maximum TEF value, 3.16, is noted for an SMST C = 7 mm at a Reynolds number of 1050. Consequently, this width is identified as the optimal width.

5.3. SMST with a helical coil wire insert

After investigating the effect of SMST width on the heat transfer and pressure drop, a width of 7 mm was chosen as the optimal width. In order to enhance heat transfer further, a HCWT was placed inside the inner tube. The results of the SMST with optimal width and HCWT were compared with the tube equipped with only the SMST and HCWT separately. The results shown in Fig. 8 demonstrate that using both SMST and HCWT turbulators together increases heat transfer by 95 % to 590 %. Using only HCWT, the increase in heat transfer ranges from 33 % to 198 %. In contrast, using the SMST with a width of 7 mm results in a heat transfer increase of 61 % to 287 % compared to a plain DTHE. These findings apply to Reynolds numbers between 8430 and1052, respectively.

Similar to the mechanisms that enhance heat transfer with the independent use of SMST, the augmentation of heat transfer through the concurrent implementation of SMST and HCWT involves decreasing the hydraulic diameter and as a result increasing the fluid velocity, creating radial flows and increasing the collision of fluid particles with the tube wall and finally weakening the thermal boundary layer. While SMST mainly affects the tube's central region, HCWT has a significant impact on the areas adjacent to the tube wall. Moreover, the findings suggest that combining SMST C = 7 mm and HCWT is most efficient at lower flow rates within the laminar flow range. For example, utilizing these two turbulators at a Reynolds number of 1052 resulted in a 590 % enhancement in heat transfer, while at a Reynolds number of 8430, the improvement observed was 95 %.

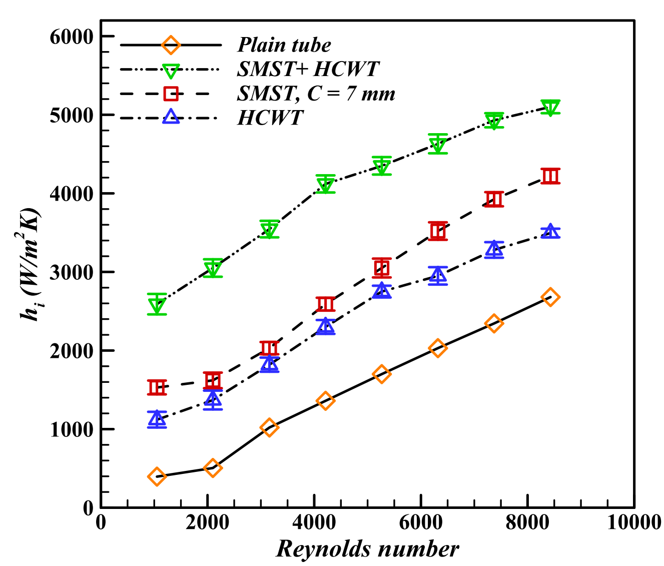

Fig. 8. h_i against Reynolds number for a tube fitted with a SMST and HCWT turbulator.

In addition to enhancing heat transfer, incorporating two types of turbulators intensifies the resistance to flow both in the tube's central area and near the tube wall. This results in a notable increase in both the pressure drop and the friction factor within the system. The ratio of friction factors f/f_0 against Reynolds number for a DTHE fitted with a SMST and HCWT turbulator is presented in Fig. 9. The increase was observed to be 3.85 to 3.15 times that of the plain DTHE configuration, 1.18 to 1.09 times that of the HCWT-equipped configuration, and 2.08 to 2.58 times that of the SMST-equipped configuration.

Given that the simultaneous use of the SMST and HCWT increased both pressure drop and heat transfer, the TEF, a dimensionless factor, was employed to determine the optimal option. The TEF at different Reynolds numbers is shown in Fig. 10. The simultaneous use of the SMST and HCWT demonstrated a synergistic effect on the thermal-frictional performance of the DTHE. A higher TEF value was observed with the combined use of SMST C = 7 mm and HCWT at Reynolds numbers below 7372. Conversely, at Reynolds numbers above 7372, a higher TEF value was observed in a heat exchanger equipped with SMST. Therefore, it is recommended to use the SMST and HCWT together for Reynolds numbers below 7372 and to use the SMST alone for Reynolds numbers above 7372. The highest TEF observed in this study reached 4.18 and was obtained when the SMST and HCWT used simultaneously at a Reynolds number of 1050.

6. Comparison against previous studies

In this investigation, the heat transfer performance was improved by changing the type of turbulator, geometry and its application. To enhance the heat transfer and TEF, HCWT was utilized alongside the SMST. The TEF at various Reynolds numbers for different heat transfer enhancement methods is shown in Fig. 11. The TEF for the SMST is 6.5 % higher than that of the magnetic turbulator with a flexible oscillator, as reported in reference [44], for the same Reynolds number. Moreover, the combination of the SMST and HCWT resulted in a significant enhancement of the TEF, with an impressive value of 4.18. The outcomes of employing HCWT alone as a passive method revealed an increase of approximately 200 % in heat transfer compared to plain DTHE, exceeding the average increase of heat transfer documented in published works from 1998 to 2022, as referenced in [3]. Additionally, comparisons have been made with other studies on passive and active methods, such as Setareh et al. [45] for the ultrasonic method, Amani et al. [46] for the MHD method, Sun et al. [47] for the EMV with multiplied vibrator, and Nakhchi et al. [48] for perforated turbulator.

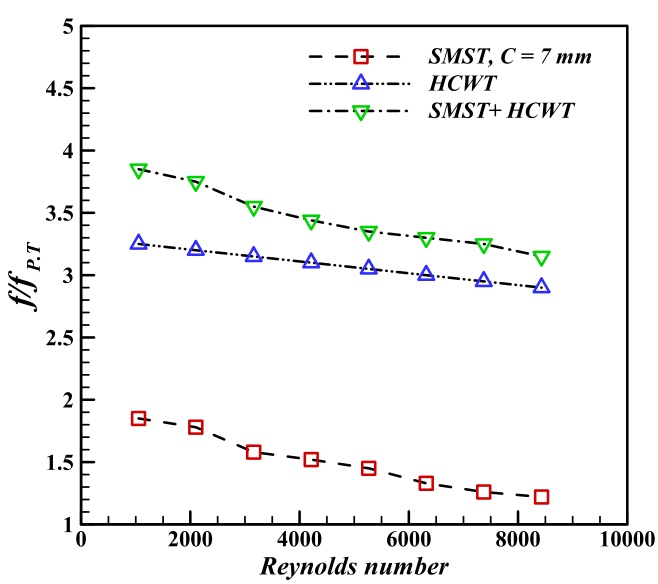

Fig. 9. f/f_0 against Reynolds number for a tube fitted with a SMST and HCWT turbulator.

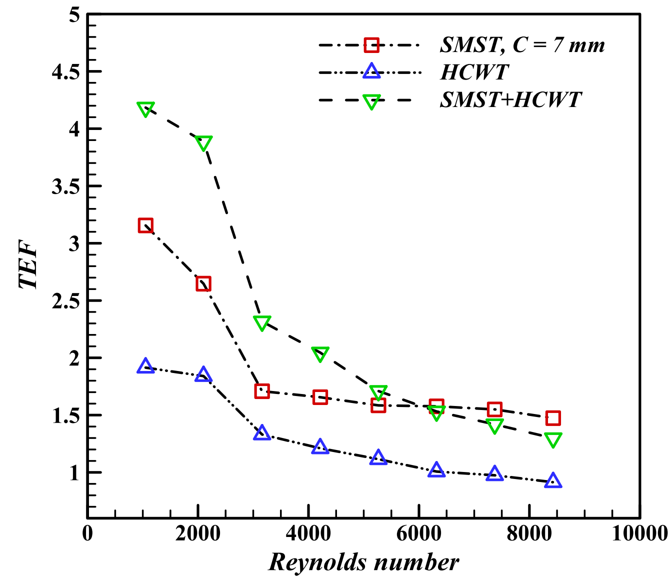

Fig. 10. TEF against Reynolds number for a tube fitted with a SMST and HCWT turbulator.

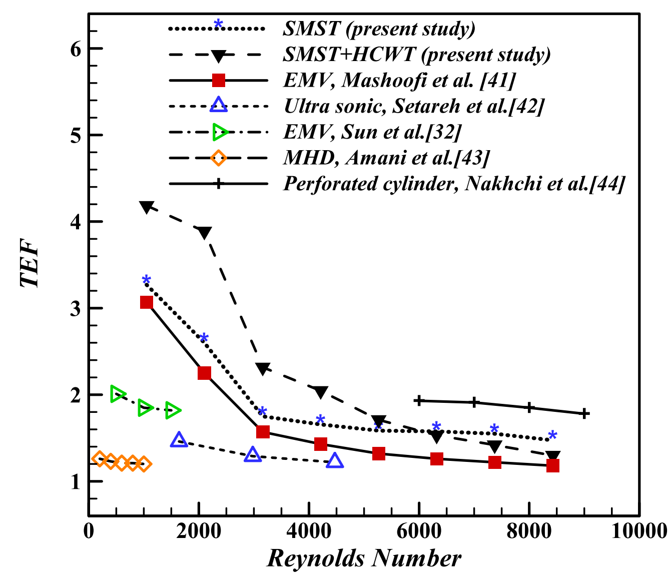

Fig. 11. Comparison of TEF against Reynolds numbers for various active and passive methods in the present study and previous research, including Setareh et al. [45], Amani et al. [46], Sun et al. [47], and Nakhchi et al. [48].

This study introduces an innovative assessment of two design techniques: SMST and HCWT. The greatest effect of the SMST, the HCWT, and their combined application on heat transfer, pressure drop, and the TEF are presented in Fig. 12. The comparison reveals that, while the combined use of two turbulators does raise the pressure drop, it substantially enhances heat transfer compared to when each turbulator is used separately. Moreover, achieving a TEF of 4.18 indicates that utilizing both an active and a passive method together can effectively improve the hydro-thermal performance of the heat exchanger.

7. Conclusions

The present investigation assessed the effect of the combined use of

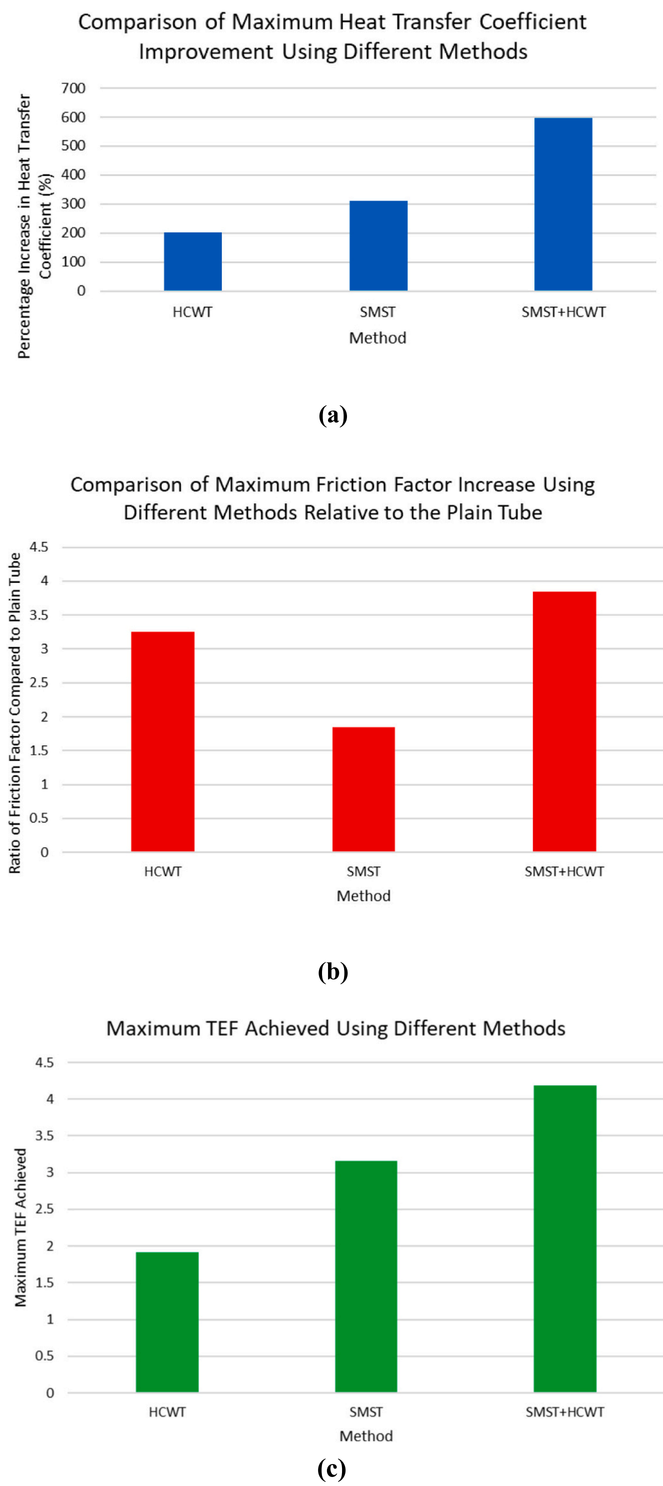

Fig. 12. The greatest effect of the SMST, the HCWT, and their combined application on (a) heat transfer, (b) pressure drop, and (c) the TEF.

SMST and HCWT on the thermal-frictional parameters of a DTHE. The examination was conducted with different SMST widths, ranging from 5 to 7 mm. The main findings of this study are:

- The use of SMST and HCWT separately increased the heat transfer by 51–311 % and 33–201 %, respectively.
- The pressure drop when using the SMST was up to 1.85 times greater than that of the plain DTHE. Similarly, with HCWT, the pressure drop increased up to 3.25 times more than the plain DTHE.
- The combined use of SMST and HCWT increased the heat transfer and pressure drop up to 6.55 times and 3.85 times, respectively, compared to those of the plain DTHE.
- The results showed that among the different strip widths examined, a width of 7 mm had a higher TEF due to its larger contact area and greater impact on the flow.
- The highest TEF recorded was 4.18, achieved using SMST and HCWT simultaneously.
- The present results suggest using the SMST on its own for Reynolds numbers higher than 7372, while for Reynolds numbers below 7372, the combined use of SMST and HCWT is recommended.

For future studies, it is suggested to evaluate the effects of the EMV method not only on heat transfer and pressure drop but also on energy consumption. This assessment should include the energy usage of both the pump and the magnetic field generator, requiring the use of variable-speed pumps to accurately measure energy consumption. Additionally, investigating various vibration frequencies and exploring different geometries for the oscillator could provide valuable insights for future research directions. It is also suggested that future studies incorporate statistical analysis to offer new insights into the EMV method and the magnetic turbulator.

Nomenclature

Symbols

A	Area, m^2
L	Tube length, m
C_p	Heat capacity, J/kg K
h	Convective heat transfer coefficient, W/m^2 K
k	Thermal conductivity, W/m K
$\dot{m}$	Working fluid flow rate, kg/s
f	Friction factor
P	Pressure, Pa
Pr	Prandtl number
Q	Heat transfer rate, J
T	Temperature, K
U	Overall heat transfer coefficient
V	Velocity, m/s
W_R	Independent variables uncertainty
W_{R+}	Dependent variables uncertainty

Subscripts

Ave	Average
c	Cold water
h	Hot water
o	Outlet
i	Inlet
ou	Outer
in	Inner
w	Water

Greek letters

Δ	Difference
μ	Dynamic viscosity, N s/m^2
ρ	Density, kg/m^3

Abbreviations

DTHE	Double tube heat exchanger
HCWT	Helically coiled wire
LMTD	Logarithmic mean temperature difference
TEF	Thermal efficiency factor

SMST Solid magnetic strip turbulator

CRediT authorship contribution statement

Nemat Mashoofi Maleki: Writing – original draft, Validation, Methodology, Formal analysis. **Saman Pourahmad:** Writing – review & editing, Writing – original draft, Software, Resources, Methodology, Formal analysis, Conceptualization. **Ebrahim Tavousi:** Writing – review & editing, Visualization, Data curation. **Noel Perera:** Writing – review & editing, Supervision, Conceptualization. **Pouyan Talebizadehsardari:** Writing – review & editing, Supervision. **Amir Keshmiri:** Supervision, Data curation.

Declaration of competing interest

The authors declare that they have no known competing financial interests or personal relationships that could have appeared to influence the work reported in this paper.

Data availability

Data will be made available on request.

References

[1] R.K. Shah, D.P. Sekulic, Fundamentals of Heat Exchanger Design, John Wiley & Sons, 2003.
[2] Y. Zhang, M. Hangi, X. Wang, A. Rahbari, A comparative evaluation of double-pipe heat exchangers with enhanced mixing, Appl. Therm. Eng. 230 (2023) 120793.
[3] E. Tavousi, N. Perera, D. Flynn, R. Hasan, Heat transfer and fluid flow characteristics of the passive method in double tube heat exchangers: a critical review, Int. J. Thermofluids 17 (2023) 100282.
[4] P. Bharadwaj, A.D. Khondge, A.W. Date, Heat transfer and pressure drop in a spirally grooved tube with twisted tape insert, Int. J. Heat Mass Transf. 52 (7) (2009) 1938–1944, https://doi.org/10.1016/j.ijheatmasstransfer.2008.08.038.
[5] T. Alam, M.-H. Kim, A comprehensive review on single phase heat transfer enhancement techniques in heat exchanger applications, Renew. Sust. Energ. Rev. 81 (2018) 813–839.
[6] G. Wang, T. Chen, M. Tian, G. Ding, Fluid and heat transfer characteristics of microchannel heat sink with truncated rib on sidewall, Int. J. Heat Mass Transf. 148 (2020) 119142.
[7] A. Alkhazaleh, F. Alnaimat, B. Mathew, Fluid flow and heat transfer behavior of a liquid based MEMS heat sink having wavy microchannels integrating circular pin-fins, Int. J. Thermofluids 20 (2023) 100480.
[8] A. Alkhazaleh, F. Alnaimat, B. Mathew, Characterization of MEMS heat sinks having straight microchannels integrating square pin-fins for liquid cooling of microelectronic chips, Therm. Sci. Eng. Progress 45 (2023) 102154.
[9] A. Alkhazaleh, F. Alnaimat, M.Y. Selim, B. Mathew, Liquid cooling of microelectronic chips using MEMS heat sink: thermohydraulic characteristics of wavy microchannels with pin-fins, Int. J. Thermofluids 18 (2023) 100313.
[10] X. Liu, et al., Thermal and hydraulic performances of the wavy microchannel heat sink with fan-shaped ribs on the sidewall, Int. J. Therm. Sci. 179 (2022) 107688.
[11] F. Alnaimat, D. Varghese, B. Mathew, Investigation of thermal and hydraulic performance of MEMS heat sinks with Zig-Zag microchannels, Int. J. Thermofluids 16 (2022) 100213.
[12] M. Omidi, M. Farhadi, M. Jafari, A comprehensive review on double pipe heat exchangers, Appl. Therm. Eng. 110 (2017) 1075–1090, https://doi.org/10.1016/j.applthermaleng.2016.09.027.
[13] W. El-Maghlany, E. Eid, M. Teamah, I. Shahrour, Experimental study for double pipe heat exchanger with rotating inner pipe, Int. J. Adv. Sci. Tech. Res. 4 (2) (2012) 507–524.
[14] Z. Zhang, Y. Ding, C. Guan, H. Yan, W. Yang, Heat transfer enhancement in double-pipe heat exchanger by means of rotor-assembled strands, Chem. Eng. Process. Process Intensif. 60 (2012) 26–33, https://doi.org/10.1016/j.cep.2012.06.003.
[15] H.H. Hamed, A.E. Mohammed, R.A. Khalefa, O.A. Habeeb, M.A. Abdulqader, The effect of using compound techniques (passive and active) on the double pipe heat exchanger performance, Egypt. J. Chem. 64 (6) (2021) 2797–2802.
[16] O. Shewale, P. Mane, S. Gazge, P. Hameed, Experimental investigation of double pipe heat exchanger with helical fins on the inner rotating tube, Int. J. Res. Eng. Technol. 3 (7) (2014) 98–102.
[17] N.M. Maleki, S. Pourahmad, Heat transfer enhancement in a heated copper tube using the electromagnetic vibration method for nanofluids as working fluid: an experimental study, Int. Commun. Heat Mass Transf. 141 (2023) 106566.
[18] Y. Tada, S. Yoshioka, A. Takimoto, Y. Hayashi, Heat transfer enhancement in a gas–solid suspension flow by applying electric field, Int. J. Heat Mass Transf. 93 (2016) 778–787.
[19] I. Kozhevnikov, M. Bologa, Influence of electrohydrodynamic flows on intensification of heat-and mass-transfer processes: Part 2. Single-and multistage electrohydrodynamic pumps, Surf. Eng. Appl. Electrochem. 58 (6) (2022) 638–656.
[20] A. Hassan, J.S. Cotton, Investigation of the role of electrohydrodynamic forces on the heat transfer enhancement and solid extraction during melting of paraffin wax under constant temperature boundary conditions, Int. J. Heat Mass Transf. 204 (2023) 123831.
[21] H. Heidary, R. Hosseini, M. Pirmohammadi, M. Kermani, Numerical study of magnetic field effect on nano-fluid forced convection in a channel, J. Magn. Magn. Mater. 374 (2015) 11–17.
[22] M. Goharkhah, M. Ashjaee, M. Shahabadi, Experimental investigation on convective heat transfer and hydrodynamic characteristics of magnetite nanofluid under the influence of an alternating magnetic field, Int. J. Therm. Sci. 99 (2016) 113–124.
[23] M. Goharkhah, A. Salarian, M. Ashjaee, M. Shahabadi, Convective heat transfer characteristics of magnetite nanofluid under the influence of constant and alternating magnetic field, Powder Technol. 274 (2015) 258–267.
[24] M. Jafari, M. Farhadi, K. Sedighi, Convection heat transfer of SWCNT-nanofluid in a corrugated channel under pulsating velocity profile, Int. Commun. Heat Mass Transf. 67 (2015) 137–146.
[25] C. Wantha, Effect and heat transfer correlations of finned tube heat exchanger under unsteady pulsating flows, Int. J. Heat Mass Transf. 99 (2016) 141–148.
[26] F. Selimefendigil, H.F. Öztop, Pulsating nanofluids jet impingement cooling of a heated horizontal surface, Int. J. Heat Mass Transf. 69 (2014) 54–65.
[27] N.M. Maleki, M. Ameri, R.H. Khoshkhoo, Experimental study of the thermal-frictional behavior of a horizontal straight tube equipped with a vibrating string turbulators: a novel active method, Exp. Thermal Fluid Sci. 140 (2023) 110767.
[28] N.M. Maleki, M. Ameri, R.H. Khoshkhoo, M. Transfer, Experimental and numerical study of the thermal-frictional behavior of a horizontal heated tube equipped with a vibrating oscillator turbulator, Int. Commun. Heat Mass Transf. 135 (2022) 106154.
[29] N.B. Khedher, S. Mehryan, M. Medani, M.M. Selim, N.B. Elbashir, M. Boujelbene, Enhancing the efficiency of a double tube heat exchanger via a novel vibrating woven wire turbulator combined with a helical coiled wire; an experimental study, Appl. Therm. Eng. 248 (2024) 123121.
[30] B. Yao, A.M. Alqahtani, W. Deebani, M. Shutaywi, S. Ghoushchi, Improving the thermal performance of the heat exchanger through simultaneous utilization of novel magnetic turbulators and helical coil wire turbulators, Int. J. Therm. Sci. 197 (2024) 108812.
[31] C. Pan, A.M. Alqahtani, H. Wei, N. Sulaiman, A.M. Elsiddieg, S. Ghoushchi, Heat transfer enhancement of a heat exchanger using novel multiple perforated magnetic turbulators (MPMT): an experimental study, Int. J. Therm. Sci. 195 (2024) 108642.
[32] A.M. Abed, et al., Heat transfer augmentation in a double pipe heat exchanger by tandem utilization of bubble injection and novel magnetic turbulators methods, Case Stud. Therm. Eng. 57 (2024) 104298.
[33] A. Zohir, M. Habib, M. Nemitallah, Heat transfer characteristics in a double-pipe heat exchanger equipped with coiled circular wires, Exp. Heat Transf. 28 (6) (2015) 531–545.
[34] E.K. Akpinar, Evaluation of heat transfer and exergy loss in a concentric double pipe exchanger equipped with helical wires, Energy Convers. Manag. 47 (18–19) (2006) 3473–3486.
[35] S. Padmanabhan, O.Y. Reddy, K.V.A.K. Yadav, V.B. Raja, K. Palanikumar, Heat transfer analysis of double tube heat exchanger with helical inserts, Mater. Today Proc. 46 (2021) 3588–3595.
[36] N.M. Maleki, M. Ameri, R.H. Khoshkhoo, Experimental and numerical study of the thermal-frictional behavior of a horizontal heated tube equipped with a vibrating oscillator turbulator, Int. Commun. Heat Mass Transf. 135 (2022) 106154.
[37] F.P. Incropera, D.P. DeWitt, T.L. Bergman, A.S. Lavine, Fundamentals of Heat and Mass Transfer, Wiley, New York, 1996.
[38] S. Pourahmad, S. Pesteei, Effectiveness-NTU analyses in a double tube heat exchanger equipped with wavy strip considering various angles, Energy Convers. Manag. 123 (2016) 462–469.
[39] N. Mashoofi, S. Pourahmad, S. Pesteei, Study the effect of axially perforated twisted tapes on the thermal performance enhancement factor of a double tube heat exchanger, Case Stud. Therm. Eng. 10 (2017) 161–168.
[40] R.J. Moffat, Describing the uncertainties in experimental results, Exp. Thermal Fluid Sci. 1 (1) (1988) 3–17, https://doi.org/10.1016/0894-1777(88)90043-X.
[41] A. Akbari, S. Kouravand, S. Pourahmad, A comprehensive study of the second law of thermodynamics for a rotary regenerative heat exchanger with two types of simple and anodized aluminum sheets: an experimental study, Energy Sources Part A (2020) 1–16.
[42] J.F. Heiss, J. Coull, Nomograph of Dittus-Boelter equation for heating and cooling liquids, Ind. Eng. Chem. 43 (5) (1951) 1226–1229.
[43] B.S. Petukhov, Heat transfer and friction in turbulent pipe flow with variable physical properties, in: Advances in Heat Transfer vol. 6, Elsevier, 1970, pp. 503–564.
[44] N. Mashoofi Maleki, S. Pourahmad, R. Haghighi Khoshkhoo, M. Ameri, Performance improvement of a double tube heat exchanger using novel electromagnetic vibration (EMV) method in the presence of Al2O3-water and CuO-water nanofluid; an experimental study, Energy 281 (2023) 128193, https://doi.org/10.1016/j.energy.2023.128193.
[45] M. Setareh, M. Saffar-Avval, A. Abdullah, Experimental and numerical study on heat transfer enhancement using ultrasonic vibration in a double-pipe heat exchanger, Appl. Therm. Eng. 159 (2019) 113867, https://doi.org/10.1016/j.applthermaleng.2019.113867.

[46] M. Amani, M. Ameri, M. Kasaeian, M. Materials, The efficacy of magnetic field on the thermal behavior of MnFe2O4 nanofluid as a functional fluid through an open-cell metal foam tube 432 (2017) 539–547.

[47] K. Sun, et al., Experimental study of the hydrothermal characteristics of copper tube in the presence of the multi-string and multi-strip magnetic turbulator, Appl. Therm. Eng. 228 (2023) 120471.

[48] P. Razi, M.A. Akhavan-Behabadi, M. Saeedinia, Pressure drop and thermal characteristics of CuO–base oil nanofluid laminar flow in flattened tubes under constant heat flux, Int. Commun. Heat Mass Transf. 38 (7) (2011) 964–971, https://doi.org/10.1016/j.icheatmasstransfer.2011.04.010.